Vol. 148: 167–181, 2022
https://doi.org/10.3354/dao03652

DISEASES OF AQUATIC ORGANISMS
Dis Aquat Org

Published online April 21

High prevalence of *Paramarteilia canceri* infecting velvet swimming crabs *Necora puber* in Ireland

Evelyn Collins[1], Georgia M. Ward[2,3], Kelly S. Bateman[3,4], Deborah L. Cheslett[1,*], Chantelle Hooper[3,4], Stephen W. Feist[3,4], Joseph E. Ironside[5], Teresa Morrissey[1], Ciar O'Toole[1], Oliver Tully[1], Stuart H. Ross[3,4], Grant D. Stentiford[3,4], Fiona Swords[1], Ander Urrutia[3], David Bass[2,3,4]

[1]Marine Institute, Rinville, Oranmore H91 R673, Ireland

[2]Department of Life Sciences, The Natural History Museum, London SW7 5BD, UK

[3]International Centre of Excellence in Aquatic Animal Health, Centre for Environment, Aquaculture and Fisheries Science, Weymouth DT4 8UB, UK

[4]Sustainable Aquaculture Futures, Biosciences, College of Life and Environmental Sciences, University of Exeter, Stocker Road, Exeter EX4 4QD, UK

[5]Institute of Biological, Environmental & Rural Sciences (IBERS), Aberystwyth University, Aberystwyth SY23 3DA, UK

ABSTRACT: The velvet swimming crab *Necora puber* has been fished in Ireland since the early 1980s and contributes significant income to smaller fishing vessels. From 2016 onwards, reduced landings have been reported. We undertook a full pathological investigation of crabs from fishing grounds at 3 sites on the west (Galway), southwest (Castletownbere) and east (Howth) coasts of Ireland. Histopathology, transmission electron microscopy and molecular taxonomic and phylogenetic analyses showed high prevalence and infection level of *Paramarteilia canceri*, previously only reported from the edible crab *Cancer pagurus*. This study provides the first molecular data for *P. canceri*, and shows its phylogenetic position in the order Paramyxida (Rhizaria). Other parasites and symbionts detected in the crabs were also noted, including widespread but low co-infection with *Hematodinium* sp. and a microsporidian consistent with the *Ameson* and *Nadelspora* genera. This is the first histological record of *Hematodinium* sp. in velvet crabs from Ireland. Four *N. puber* individuals across 2 sites were co-infected by *P. canceri* and *Hematodinium* sp. At one site, 3 velvet crabs infected with *P. canceri* were co-infected with the first microsporidian recorded from this host; the microsporidian 18S sequence was almost identical to *Ameson pulvis*, known to infect European shore crabs *Carcinus maenas.* The study provides a comprehensive phylogenetic analysis of this and all other available *Ameson* and *Nadelspora* 18S sequences. Together, these findings provide a baseline for further investigations of *N. puber* populations along the coast of Ireland.

KEY WORDS: *Paramarteilia orchestiae* · Paramyxida · *Cancer pagurus* · *Hematodinium* · Microsporidia · *Ameson pulvis* · Amphipod · Crab

1. INTRODUCTION

The velvet swimming crab *Necora puber* has a wide distribution along the rocky coasts of the eastern Atlantic, extending from Norway south along the French and Spanish coast to North Africa as well as in the eastern Mediterranean (Christiansen 1969, Bakir & Healy 1995). In Ireland, the species occurs in all coastal waters, but fishing of *N. puber* only commenced in the early 1980s in response to the market demand created by declines in landings in France and southern Europe. During the period 2004–2019, landings in Ireland varied between 150 and 400 t. The majority of *N. puber* are caught as by-catch in

*Corresponding author: deborah.cheslett@marine.ie

Publisher: Inter-Research · www.int-res.com

the lobster fishery, and are an important source of income to many smaller (<8 m) inshore vessels which form the bulk (approximately 55%) of the commercial fleet. Over 80% of velvet crabs are landed by vessels under 10 m in length, with these landings valued at €0.67 million distributed across over 200 vessels in 2019 (Marine Institute & Bord Iascaigh Mhara 2019).

In spring 2016, reports of a decline in landings of *N. puber* were received from fishermen operating in Galway Bay who observed that catches of juvenile crabs were plentiful but few adult crabs were being caught. This prompted an investigation into the possible causes through a preliminary histopathological survey of crabs sampled from both inner and outer Galway Bay. The histopathological survey revealed a high prevalence and intensity of infection with a paramyxid parasite with morphology and pathognomonic signs concordant with *Paramarteilia*. A follow-up histopathological survey was conducted in this and a further 2 additional fishing grounds to determine the distribution of the parasite in the Irish *N. puber* fishery. *Paramarteilia* belongs to the order Paramyxida (Ascetosporea, Rhizaria), which comprises protistan parasites of marine invertebrate hosts including molluscs, crustaceans and annelid worms. *Paramarteilia* is to date the only paramyxid genus known exclusively from crustacean hosts. The genus comprises 2 described species, *P. orchestiae* and *P. canceri*, infecting amphipod and crab hosts, respectively, both described from sites in the English Channel (Feist et al. 2009).

P. canceri has only been observed infecting edible crabs *Cancer pagurus*. A similar species has been observed infecting spider crabs *Maja squinado* collected in Cardigan Bay, Wales, UK (Ward et al. 2016). *In situ* hybridisation using a *Paramarteilia*-specific 18S-targeted probe confirmed that both parasites belong to the genus *Paramarteilia*, but insufficient data were available to confirm the identity of the spider crab parasite. *P. orchestiae* has been shown to infect amphipod hosts, including the type host *Orchestia gammarellus* (Ginsburger-Vogel et al. 1976, Ginsburger-Vogel & Desportes 1979) and *Echinogammarus marinus* (Short et al. 2012, Ward et al. 2016). Cells of a parasite morphologically concordant with *Paramarteilia* have also been observed in the amphipods *O. aestuarensis* and *O. meditteranea* (Ginsburger-Vogel 1991), and this has since been confirmed by PCR screens of *O. aestuarensis* (Pickup & Ironside 2018).

Histopathology, transmission electron microscopy (TEM) and molecular taxonomic and phylogenetic analyses of a paramxyid parasite infecting *N. puber* from Galway Bay confirm this to be *P. canceri* previously detected infrequently in *C. pagurus*, for which the first molecular data are provided. Co-infection with 2 other parasites, namely a microsporidian in the genus *Ameson*, and *Hematodinium* sp., the latter previously detected in *N. puber*, but only once from Ireland (Donegal), in 2006, and at very low prevalence, is also described.

2. MATERIALS AND METHODS

2.1. Sample collection and processing

Using baited pots, we collected a total of 620 velvet swimming crabs from 3 of the main fishing grounds in the region during 2 sampling periods: February to April 2016 from Galway Bay (centroid 53° 10′ 10.9″ N, 9° 9' 16.8" W; inner bay n = 140; outer bay n = 30); and September 2017 to July 2018 from Howth (53° 23′ 5.9″ N, 6°3'12.5'' W; n = 150), Galway Bay (n = 150) and Castletownbere (centroid 51° 39′ 4.8″ N, 9° 42′ 16.0″ W; n = 150) (Fig. 1). On arrival in the laboratory, the crabs appeared healthy and displayed no external signs of disease, lethargy or unresponsiveness, and minimal biofouling. Internally, the tissues and organs did not appear affected by disease. Little variation in mean carapace width was observed between samples (between 72.30 and 77.88 mm). A higher ratio of male to female velvet crabs was sampled (431:189, across all samples).

Crabs were placed on ice for a minimum of 30 min to anaesthetise them before dissection. Samples of heart, hepatopancreas, gill, gonad, cuticular epithelium and muscle were removed from each crab and placed into Davidson's seawater fixative for histology and 100% ethanol for molecular analyses. Nerve tissue, tegmental gland and antennal gland were also sampled from some individuals for histology. Additional samples of hepatopancreas, muscle, cuticular epithelium and gill were placed into 2.5% glutaraldehyde in 0.1 M sodium cacodylate buffer for electron microscopy. The samples of edible crab used in this study were those collected by Feist et al. (2009).

In Ireland, amphipods (*Orchestia* sp.) were collected from the shoreline in inner Galway Bay (sample set 'GAL'). Amphipods were chilled on ice for a minimum of 15 min and cut in half transversally. The lower body was placed into Davidson's seawater fixative for histology and the head and anterior part of the thorax were placed directly into lysis buffer (QIAamp DNA Mini Kit, Qiagen) prior to DNA extraction.

In southern England, amphipods were collected as follows: *Jassa* sp. from the National Lobster Hatchery, Padstow, Cornwall, in March 2017 (sample set

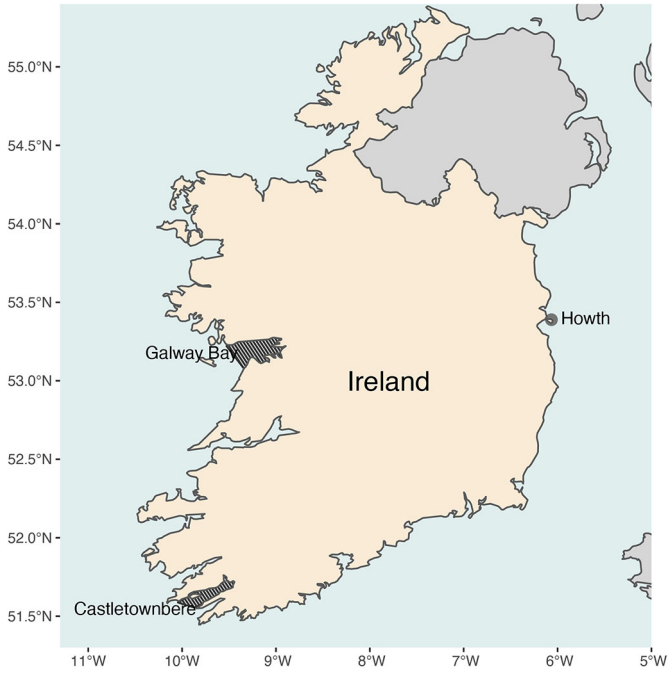

Fig. 1. Fishery areas (dark shading) in Ireland sampled for this study

RA17017), *Orchestia* sp. from Jupiter Point on the Lynher River (Tamar Estuary), Devon, in November 2018 (RA18098) and *Echinogammarus marinus* from Jupiter Point in April 2017 and November 2018 (RA17028 and RA18098). All were processed for histology, TEM and molecular analyses as described by Urrutia et al. (2019).

Orchestia spp. were also collected from a range of locations to investigate as far as practical the identity/diversity of *Paramarteilia* infecting them: from the Penzé Estuary, France, and the Gann Estuary, Pembrokeshire, Wales, UK, and processed as reported by Pickup & Ironside (2018) (sample sets TB and DOM). A further sample set of *Orchestia* sp. was collected from the Gann Estuary in November 2019 (sample set GANN) and preserved in 100% ethanol for DNA extraction.

2.2. DNA extraction

DNA was extracted from *Necora puber* and Irish amphipod tissue using the QIAamp DNA Mini Kit (Qiagen) with a Qiagen QIAcube robot according to the manufacturer's protocol, and from amphipods from sites in southern England and sample set GANN using a phenol:chloroform protocol as in Urrutia et al. (2019). Sample sets TB and DOM are reported in Pickup & Ironside (2018).

DNA was extracted from sections of wax-embedded tissues of *Cancer pagurus* infected with *P. canceri* using the EZNA FFPE DNA Kit (Omega Biotek). Following extraction, DNA was quantified using a Qubit High Sensitivity dsDNA assay kit (Life Technologies), before extracted DNA (5 ng) was repaired using the NEBNext FFPE DNA Repair Mix (New England Biolabs).

2.3. PCR and sequencing

The sequences of all primers used for the amplification of *Paramarteilia* 18S and first internal transcribed spacer (ITS1) from crabs and amphipods are given in Table 1. The V7-V8 regions (ca. 400 bp) of the paramyxid 18S rRNA gene were amplified using nested primer set B (Para1fGW/ParaGENrGW, followed by Para3fGW/ParaGENrGW) and reaction conditions of Ward et al. (2016). The full ITS1 region was amplified using primers PMart_18S_For and PMart_58S_Rev, producing an approximately 650 bp amplicon from the V9 hypervariable region of the 18S rRNA gene to the 5.8S rRNA gene. Reaction mixtures had a final volume of 20 µl and comprised 0.5 µM of each primer, 2.5 mM $MgCl_2$, 0.4 mM dNTPs, 0.2 mM bovine serum albumin (BSA), 0.5 U GoTaq Flexi polymerase (Promega) and 1 µl of extracted DNA as template. Reaction conditions consisted of an initial 5 min denaturation at 95°C; 35 amplification cycles at 95°C for 1 min, 62°C for 1 min

Table 1. PCR primers used in this study to amplify *Paramarteilia* and microsporidian lineages

Primer	Sequence (5′–3′)	Target region	Reference
Para1fGW (R1 forward)	GGG CGA GGG GTA AAA TCT	Paramyxid 18S	Ward et al. (2016)
ParaGENrGW (both rounds reverse)	GTG TAC AAA GGR CAG GGA CT		
Para3fGW (R2 forward)	GGC TTY TGG GAG AKT ACG GC		
PMart_18S_For	GAG CCG GAA AGT CAC TGA GCG	*Paramarteilia* ITS1	This study
PMart_58S_Rev	GAC GCC GCG ATT TGC TTT CGG A		
CTMicrosp	CAC CAG GTT GAT TCT GCC TGA CG	Microsporidian 18S	Stentiford et al. (2018)
Microsp1342r	ACG GGC GGT GTG TAC AAA GAA CAG		

and 72°C for 1 min; and a final extension at 72°C for 10 min before storage at 4°C. Resultant amplicons from both 18S and ITS1-targeted PCRs were visualised on 2% agarose gels stained with GelRed (Biotium), before Sanger sequencing using the respective forward primer. Primer sequences and low-quality base pairs were trimmed from chromatograms using Geneious R11.

Partial microsporidian 18S sequences (approximately 1200 bp) were amplified from infected *N. puber* tissues from 3 infected individuals using the microsporidian-specific primer set and cycling conditions of Stentiford et al. (2018). Reaction composition was as for *Paramarteilia*, but did not include BSA.

2.4. Phylogenetic analyses

2.4.1. 18S phylogeny of paramyxids

All known paramyxid 18S sequence types were subject to BLASTn searches against the NCBI GenBank database to retrieve additional (including uncharacterised and environmental) sequence types showing high (>80%) coverage and sequence identity (>90%). Where identical 18S sequences were available for the same species, the longest sequence was retained for phylogenetic analyses. We trimmed 35 bp from each end of the retrieved *P. orchestiae* 18S sequences to remove potentially artifactual diversity close to primer sites, and the representative sequence JQ673484 was used for analysis. These sequences (including the haplosporidian outgroup) were added to those generated in this study from *N. puber*, *C. pagurus* and amphipods, and aligned using the MAFFT (version 7) E-INS-i algorithm (Katoh & Standley 2013) and refined by eye. The resulting 18S alignment was used for maximum likelihood analysis in RAxML BlackBox Version 8 (Stamatakis 2014), using a generalised time-reversible model with CAT approximation. The proportion of invariable sites was estimated from the data, and a rapid bootstrapping model was employed. Bootstopping was not used, and the consensus tree was constructed from 1000 bootstrap iterations. Bayesian consensus trees were constructed using MrBayes Version 3.2.7 (Ronquist et al. 2012). Two separate MC^3 runs with randomly generated starting trees were carried out for 2 million generations each, with 1 cold and 3 heated chains, an equal substitution model and a temperature parameter of 0.2. The first 500 000 generations were discarded as burn-in, and trees were sampled every 1000 generations. Majority rule consensus trees were constructed from the remaining samples. All maximum likelihood and Bayesian phylogenetic analyses were performed in the CIPRES server (Miller et al. 2010).

2.4.2. ITS1 phylogeny of *Paramarteilia*

ITS1 *Paramarteilia* sequences (n = 62) generated from crab and amphipod tissues were aligned with existing ITS1 sequence data for European *Marteilia* spp. using MAFFT (version 7) L-INS-i algorithm (Katoh & Standley 2013) and refined by eye. Because of the high degree of similarity between *Paramarteilia* ITS1 sequences, which lack a phylogenetic signal suitable for sophisticated models, this alignment was analysed using simple distance matrices and parsimony methods, all of which gave similar results. The tree shown (see Fig. 6) uses the maximum parsimony optimality criterion with a branch-and-bound analysis search, ignoring gaps. The sequence order was randomized 5 times, and 1000 bootstraps were performed. Analyses were carried out in SeaView (Gouy et al. 2010). ITS1 sequence signatures unique to crab- and amphipod-derived *Paramarteilia* isolates were identified by visual inspection of the aligned datasets, and their positions determined relative to MZ366973 (RA18098-01). Sequences were submitted to NCBI GenBank under accession numbers MZ366959 to MZ367020.

2.4.3. 18S phylogeny of *Ameson* and *Nadelspora* spp. (Microsporidia)

All available 18S sequences from representatives of these 2 very closely related genera were downloaded from GenBank and aligned as described above with the new sequence generated from the microsporidian infecting *Necora* in this study. Maximum parsimony analyses were carried out as described above for the *Paramarteilia* ITS1 alignment.

2.5. Histology and TEM

2.5.1. Histology

Samples were fixed in Davidson's seawater fixative for a minimum of 24 h before transfer to 70% ethanol (Tecnisolv). Fixed samples were processed to wax in a vacuum infiltration processor (Leica Peloris / Leica ASP 200S) using standard protocols. Sections were cut at a thickness of 3–5 µm on a rotary microtome and were mounted onto glass slides before staining

with haematoxylin and eosin (H&E). Tissues and organs from *N. puber* were also stained with periodic acid-Schiff (PAS) and Feulgen stains. Stained sections were analysed by light microscopy (Nikon Eclipse Ni), and digital images were taken using the NIS-Elements Imaging Software (Nikon).

2.5.2. TEM

Tissues and organs were fixed in 2.5% glutaraldehyde in 0.1 M sodium cacodylate buffer for 1 h, rinsed in sodium cacodylate buffer, then post-fixed in 1% osmium tetroxide in sodium cacodylate buffer. Samples were rinsed in sodium cacodylate buffer before being dehydrated through a graded acetone series and embedded within Agar 100 epoxy resin (Agar Scientific). Semithin sections (1–2 µm) were stained with toluidine blue to identify suitable target areas. Ultrathin sections (70–90 nm) of these areas were mounted on uncoated copper grids and stained with aqueous uranyl acetate and Reynolds lead citrate (Reynolds 1963). Samples were examined with a JEOL JEM 1400 transmission electron microscope, and digital images were captured using an AMT XR80 camera and AMTv602 software.

3. RESULTS

3.1. Histology

3.1.1. *Paramarteilia*

A total of 620 *Necora puber* were examined for the presence of pathogens. Over the study period, the most prevalent parasite infection recorded in all 3 bays was a *Paramarteilia* sp. (Table 2). Galway Bay had the highest prevalence with 160 crabs infected out of the 320 sampled (50%). Infected crabs revealed a systemic invasion of most organs and tissues by this parasite. *Paramarteilia* cells were observed throughout the connective tissues and within cells of numerous organs and other tissues of infected crabs. In the heart, *Paramarteilia* cells were observed both within the sarcolemmal space surrounding muscle bundles and in spongy pericardium. Parasite cells were also observed within epithelial cells of the tegumental gland and within nervous tissues. In the ovary, parasites were detected within cells of the connective tissue surrounding developing oocytes and within apparently viable oocytes themselves. In the testis, parasite cells were observed within cells of the connective tissues surrounding the tubules and within epithelial cells surrounding the seminiferous tubules (Fig. 2). Parasites were often concentrated within the antennal gland; in advanced infections, desquamated antennal gland epithelium and unidentified concretions intermixed with masses of parasite life stages within the tubule lumens. Parasite life stages within the antennal gland were often magenta in colour when stained with PAS, indicating accumulations of glycogen in these cells. Feulgen staining demonstrated the characteristic presence of multiple nuclei within a well-defined 'cell-within-cell' arrangement typical of paramxyid parasites (Fig. 3).

3.1.2. Other parasites

A microsporidian was also observed infecting the musculature of 3 *Paramarteilia*-infected *N. puber* from Galway Bay. Various developmental stages of the microsporidian displaced or replaced normal myofibrils of the skeletal musculature. Myofibres within the heart also appeared densely stained, similar to those described by Stentiford et al. (2013), where *Nadelspora*-like spores were proposed to be a component of the *Ameson* genus life cycle. In advanced infection, the majority of the skeletal musculature was replaced by ovoid microsporidian spores. Microsporidian spores were also observed within the haemolymph of infected crabs, presumably arising from ruptured muscle fibres (Fig. 4).

Table 2. External features and infection type/prevalence of velvet crab samples from inner and outer Galway Bay, Howth and Castletownbere, Ireland. CW: carapace width (mean ± SD); M:F: male to female ratio

Location, year(s)	n	CW (mm)	M:F	Crabs with symbionts (%)			
				Biofouling	*Paramarteilia*	*Ameson*/*Nadelspora*	*Hematodinium*
Inner Galway Bay (2016)	141	77.9 ± 9.5	118:22	49 (35)	67 (48)	3 (2)	5 (4)
Outer Galway Bay (2016)	30	77.8 ± 8.0	20:10	3 (10)	9 (30)	0	1 (3)
Galway Bay (2017–18)	150	70.6 ± 8.0	108:42	7 (4.7)	84 (56)	0	3 (2)
Howth (2017–18)	150	71.6 ± 6.0	88:62	22 (14.7)	7 (5)	0	10 (7)
Castletownbere (2017–18)	150	72.5 ± 5.6	97:53	4 (2.7)	20 (13)	0	6 (4)

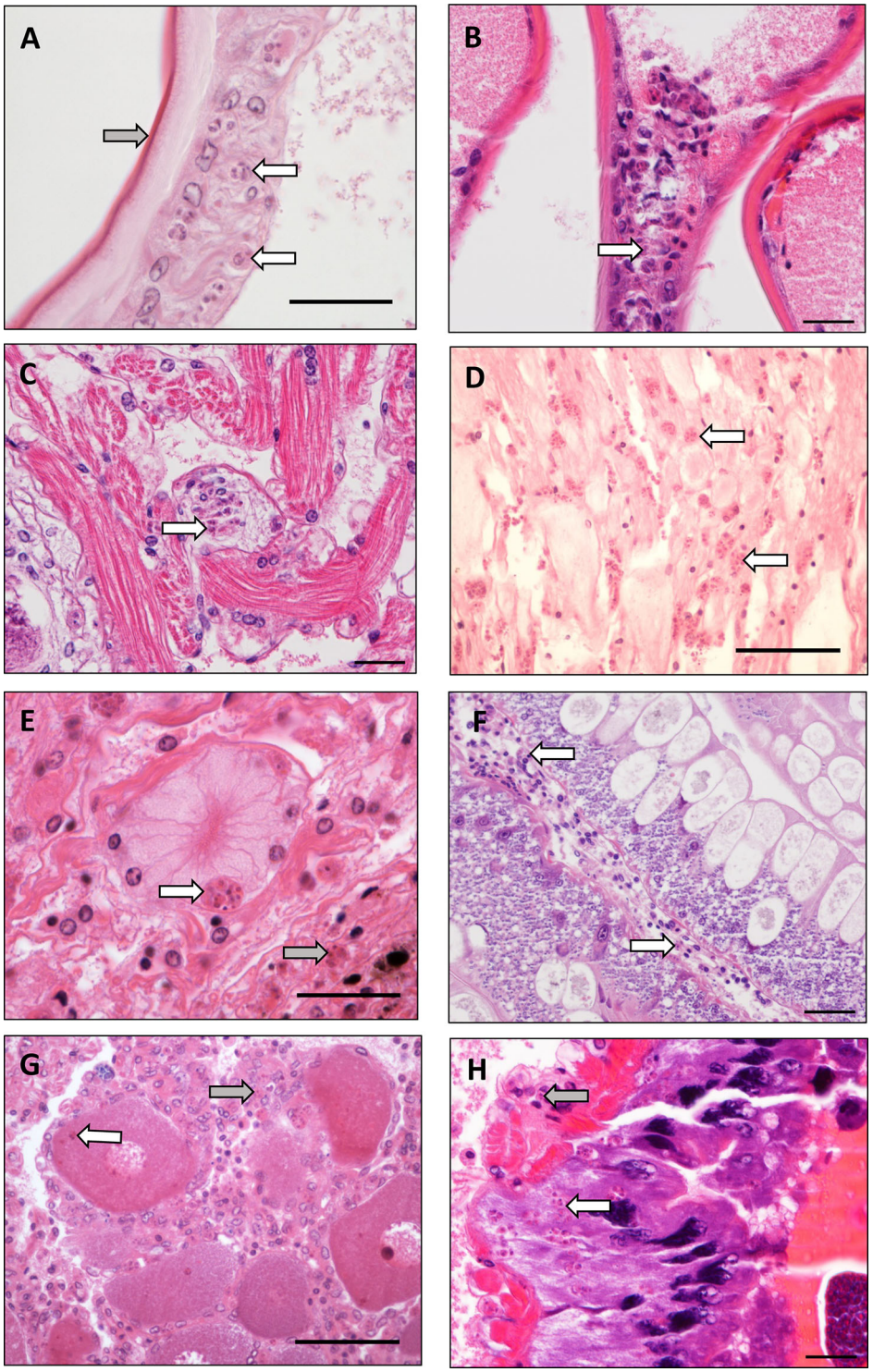

Fig. 2. *Paramarteilia* sp. infection of *Necora puber*. (A) Parasites (white arrows) within cuticular epithelial cells immediately beneath the cuticle (grey arrow). (B) Parasites (arrow) within connective tissue of gill filaments. (C) Parasites (arrow) in the connective tissues surrounding the muscle bundles within the heart. (D) Parasites frequenting the ventral and peripheral nerves (arrows). (E) Parasites infecting the cytoplasm of tegmental gland cells (white arrow) and within widely dispersed connective tissues of the host (example, grey arrow). (F) Parasites (arrow) were observed in the connective tissues surrounding the tubules of the hepatopancreas. (G) Parasites were observed within the cytoplasm of apparently viable oocytes (white arrow) and in connective tissues of the ovary (grey arrow). (H) Parasites were observed within the connective tissues (fibrous capsule) surrounding the seminiferous tubules (grey arrow) of the testis. Parasites were also observed within the epithelium (white arrow) of the seminiferous tubules. All images H&E stain. Scale bars = (A–C, E, H) 25 µm; (D, F, G) 50 µm

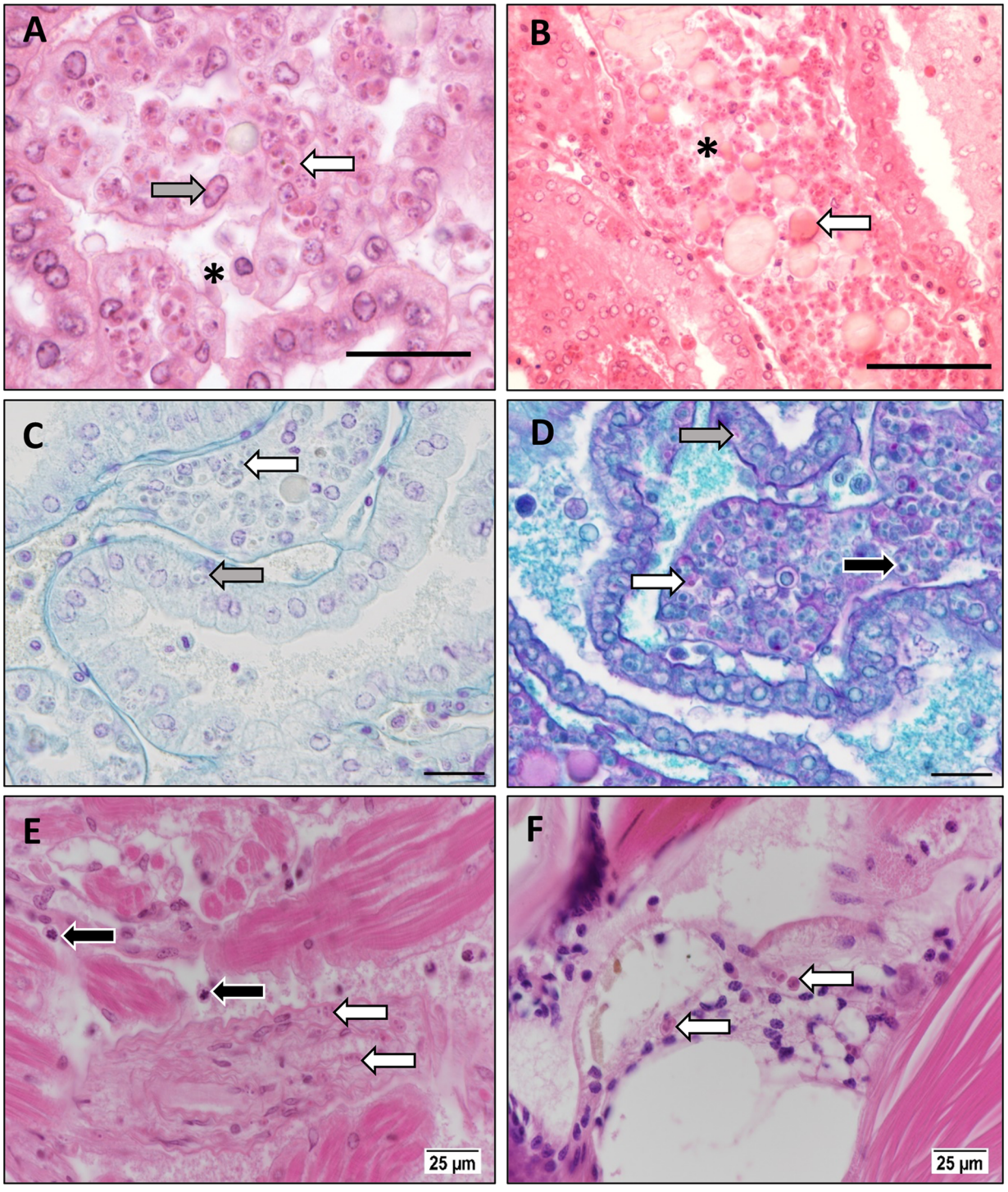

Fig. 3. *Paramarteilia* sp. infection of (A–E) *Necora puber* and (F) *Orchestia gammarellus*. (A) Highest abundance of parasites was observed within haemal spaces (asterisk) and within tubules (white arrow) of the antennal gland. The gland appeared atrophic with separation of bladder epithelial cells from basement membranes and exposure of host cell nuclei (grey arrow). H&E stain. (B) In late stage infection, desquamated antennal gland (bladder) epithelium and unidentified concretions (arrow) intermixed with masses of parasite life stages (asterisk). H&E stain. (C) Parasites were observed within haemal spaces (white arrow) and within tubules (grey arrow) of the antennal gland. Cell-within-cell arrangement can be clearly seen with Feulgen staining, with nuclei of the parasite staining red. (D) Parasites within haemal spaces (black arrow) and within tubule epithelium (grey arrow) of the antennal gland; some development stages stain red (white arrow) with periodic acid-Schiff stain, indicating presence of glycogen. (E) Co-infection of *Necora puber* with *Paramartelia* sp. (white arrows) and *Hematodinium* sp. (black arrows) within heart tissues. H&E stain. (F) *Paramarteilia* sp. parasites (arrows) within connective tissues of the amphipod *Orchestia gamarellus*. H&E stain. All scale bars = 25 µm

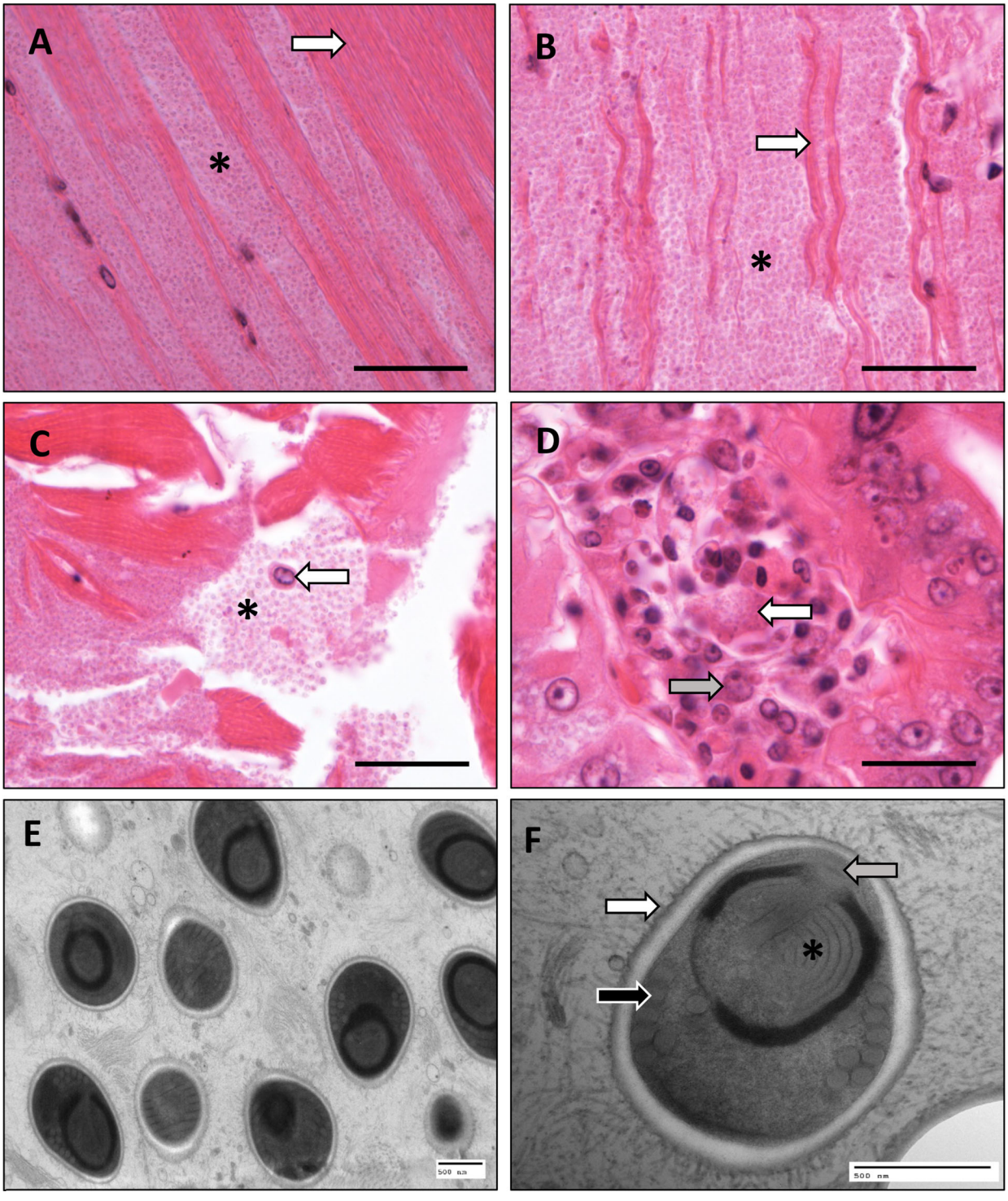

Fig. 4. *Ameson* sp. microsporidian infecting the musculature of *Necora puber*. (A) Infected skeletal myofibres are filled with masses of parasite life stages (asterisk). Uninfected fibres are relatively eosinophilic (arrow). (B) In late-stage infection, the majority of the skeletal musculature is replaced by parasite life stages (here, mainly spores; asterisk), leaving infrequent myofibrilar islands (arrow). (C) Microsporidian spores are liberated (to the haemolymph) from detached muscle fibres and blocks (asterisk). Host haemocyte (arrow) provides scale to the small microsporidian spores. (D) Infected myofibres within the heart appeared densely stained (white arrow). Co-infection with *Paramarteilia* sp. shown (grey arrow). (E) Microsporidian spores within skeletal muscle tissue. (F) Microsporidian spore containing 7–8 turns of the polar filament (black arrow), clear anchoring disc (grey arrow) and polaroplast (asterisk). Spores appear to have projections protruding from the exospore (white arrow). Images A–D: H&E stain, images E and F: TEM. Scale bars = (A–D) 25 µm; (E, F) 500 nm

A *Hematodinium* sp. was observed by histology in *N. puber* sampled from all 3 bays: Galway Bay, 9/320 (2.8%); Howth, 10/150 (6.7%); and Castletownbere, 6/150 (4%) (Table 2). The prevalence noted was low, although the prevalence in Howth was higher than that noted for *Paramarteilia* sp. Four *N. puber* were identified with co-infections of both *Paramarteilia* sp. and *Hematodinium* sp.: 3 crabs from Galway Bay and a single crab from Castletownbere. Masses of *Hematodinium* sp. parasite life stages were observed in the haemolypmh of the heart, gills and sinuses of the hepatopancreas (Fig. 3), with *Paramarteilia* sp. co-infections present throughout the connective tissues of these organs as described above.

Other incidental histological findings (not shown) included stalked ciliates commonly observed on the gills often associated with other gram-negative fouling bacteria. Metacercarial cysts were also randomly seen in the internal organs, including the heart, antennal gland and gills. Other organisms observed in very low numbers included yeast-like cells in the heart, isopod parasites distributed within the lumen of the antennal gland, adjacent to the labyrinth cells and larval nematodes attached the outer surface of gill filaments. Haplosporidian-like plasmodia were seen in the heart and testes of 1 crab, similar in appearance to the infection recently described by Davies et al. (2020) in European shore crabs.

3.1.3. Infections of amphipods

Histological examination of H&E-stained longitudinal sections revealed the presence of *Paramarteilia* sp. in 4 of 20 amphipods collected in Ireland. A similar prevalence (5/27) was observed in *Orchestia* sp. sampled in the south of England (RA18098). *Paramarteilia* infections of *Jassa* sp. sampled from Padstow were seen in 16/38 individuals. Parasites could be observed within the connective tissue cells beneath the cuticular epithelium and associated with various internal organs, including antennal and tegumental glands, gonads and gill (early stages) (Fig. 3). Tissue tropism in *Necora* and amphipods was generally similar.

3.2. TEM

The ultrastructure of the *Paramarteilia* parasites infecting *N. puber* was compared with data previously collected from infected *Cancer pagurus* (Feist et al. 2009), and is summarised in Table 3. Developmental stages of the parasite were dispersed throughout the host tissues, especially within the connective tissue cells surrounding the hepatopancreas tubules. The cell-within-cell arrangement, characteristic of this taxon, was clearly observed in parasites from both crab species, with primary cells containing secondary cells, bacilliform haplosporosomes, vacuoles and multivesicular bodies as previously described. Secondary cells contained tertiary cells, which in turn contained quaternary cells. Bacilliform haplosporosomes were identified within primary cells (Fig. 5), but appeared to be absent from secondary cells. Both bacilliform and bulb-shaped haplosporosomes were identified within the tertiary cells (Fig. 5), but were apparently absent from quaternary cells, although the sample number was too low to determine whether this is generally true. The number of secondary and tertiary cells reported in each of the crab species showed variation (Table 3).

TEM of skeletal muscle tissues infected by the microsporidian parasite revealed oval microsporidian spores containing 7–8 turns of the polar filament terminated by an anchoring disc. Spores possessed projections from the exospore surface layer and measured (mean ± SD) approximately 1.27 ± 0.14 nm × 1.01 ± 0.09 nm (n = 20) (Fig. 4), although it should be noted that spore size measurements are notoriously unreliable,

Table 3. Ultrastructural features of *Paramarteilia canceri* infections observed in velvet and edible crabs, detailing the numbers of secondary, tertiary and quaternary cells observed (4 is the maximum number recorded) and type of haplosporosomes present within these cells (see Fig. 2)

		Velvet crab *Necora puber*	Edible crab *Cancer pagurus*
1° cell	Haplosporosome type	Bacilliform	Bacilliform
2° cell	Number of cells	3	2
	Haplosporosome type	No haplosporosomes	No haplosporosomes
3° cell	Number of cells	2	4
	Haplosporosome type	Bacilliform & bulb-shaped	Bacilliform & bulb-shaped
4° cell	Number of cells	2	4
	Haplosporosome type	No haplosporosomes	No haplosporosomes

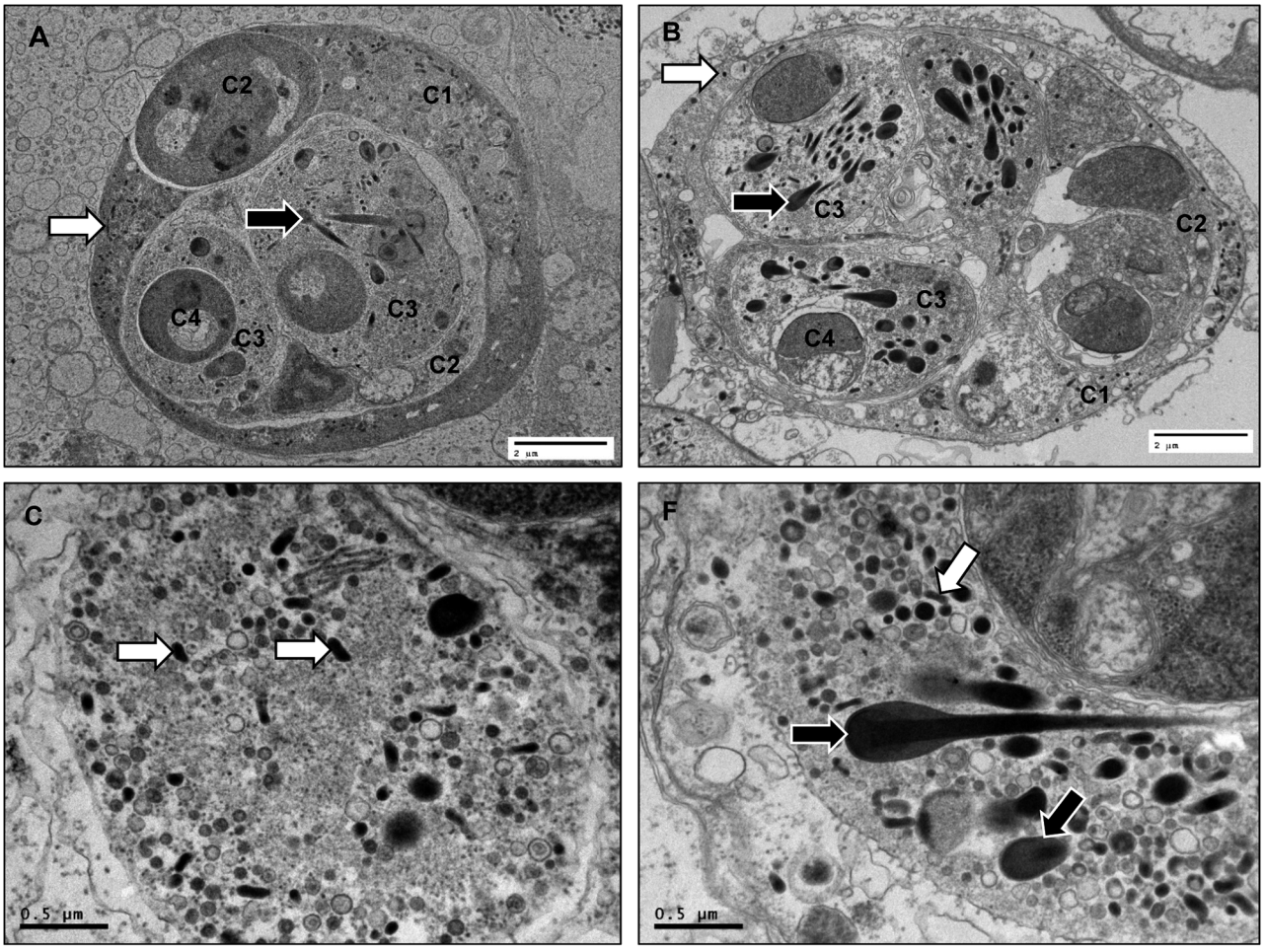

Fig. 5. Multicellular stages of *Paramarteilia canceri* within *Necora puber* and *Cancer pagurus* tissues. (A) *P. canceri* within velvet crab tissues. Cell-within-cell arrangement is clearly displayed; primary cell (C1) contains 2 secondary cells (C2). One of these secondary cells contains tertiary (C3) and quaternary cells (C4). C1 possesses bacilliform haplosporosomes (white arrow) within the cytoplasm; C3 cells display bacilliform and bulb-shaped haplosporosomes (black arrow) within the cytoplasm. (B) *P. canceri* within type host, *C. pagurus*, tissues. C1, C2, C3 and C4 cells are evident, bacilliform haplosporosomes (white arrow) are present in the cytoplasm of C1, and bacilliform and bulb-shaped haplosporosomes (black arrow) are evident in C3. (C) Bacilliform haplosporosomes (arrows) within C3 of *P. canceri*. (D) Bulb-shaped haplosporosomes (black arrows) within C3 of *P. canceri* from *C. pagurus*. Bacilliform haplosporosomes (white arrow) can also be seen. All images TEM. Scale bars = (A, B) 2 µm; (C, D) 0.5 µm

due to the effects of fixation (Parker & Warner 1970). Heart tissues were not available for electron microscopy, so it was not possible to confirm the presence of microsporidian spores within the heart myofibres.

3.3. 18S and ITS1 rDNA phylogenies

Forty-one *Paramarteilia* ITS1 sequences were generated from 37 *Orchestia* individuals from Wales (n = 19), England (n = 10), France (n = 4) and Ireland (n = 4), and *Echinogammarus* and *Jassa* from England (n = 4). Phylogenetic analysis showed that these formed a clade (labelled 'amphipods' in Fig. 6) to the exclusion of all crab-derived sequences (labelled 'crabs'). *Paramarteilia* ITS1 sequences from infected *N. puber* obtained from Galway (20 individuals) plus 1 sequence from FFPE-preserved material from the *C. pagurus* individual from which *P. canceri* was originally described (without molecular data) by Feist et al. (2009), formed a maximally supported clade comprising only crab-derived sequences.

Across the 452 bp length of the *Paramarteilia* ITS1 alignment, 13 invariant sites distinguished the amphipod and crab clades, i.e. at these sites, the clades consistently differed as follows (using MZ366973

[RA18098-01] as a reference in the format amphipod/crab): position 17: G/A, positions 47 and 56: T/C, position 103: T or C/G, positions 111–113: CTG/TCC, position 131: G/A, position 180: A/T, position 269: T/C, position 278: G/A, positions 321 and 393: T/C. At position 177, all amphipod and 12 of the crab-derived sequences had A, except 8 or 9 crab-derived sequences, which had a G.

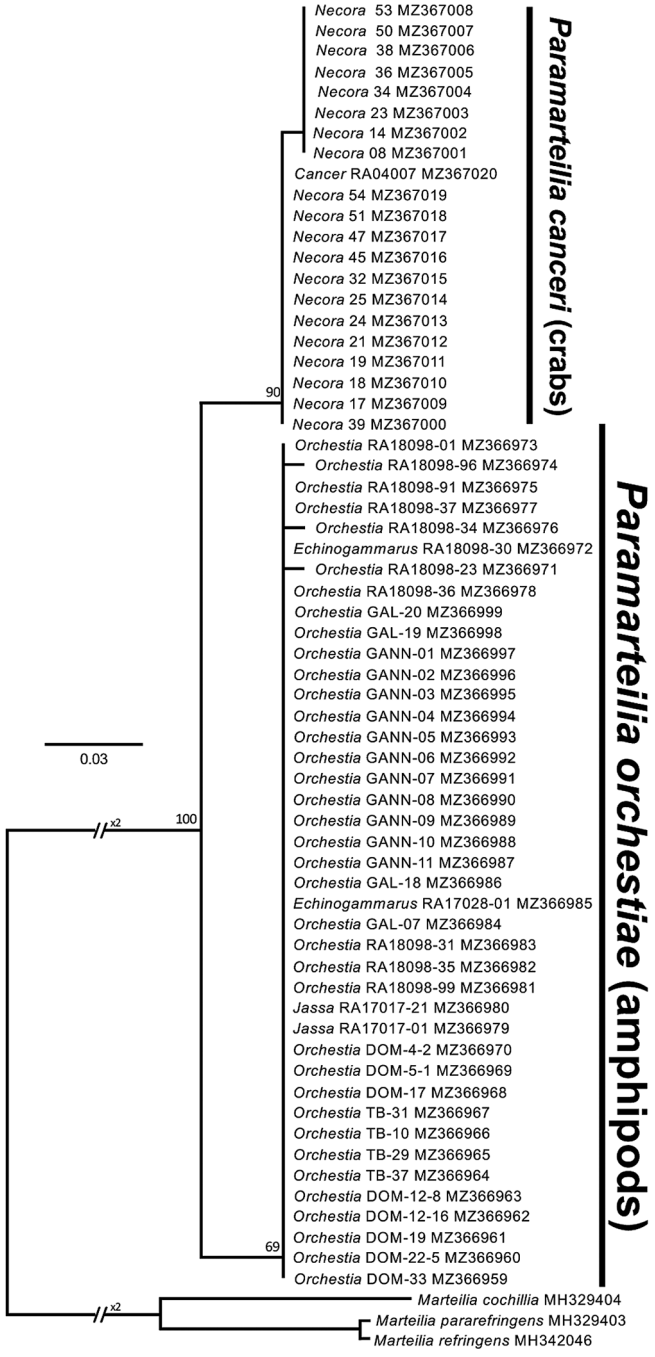

Fig. 6. ITS1 rDNA maximum parsimony phylogeny (1000 bootstrap replicates; bootstrap percentages given at nodes) of 18 amphipod-derived and 41 crab-derived *Paramarteilia* sequences, corresponding to *P. orchestiae* and *P. canceri*, respectively, which form mutually exclusive clades. See Section 3.3 for an analysis of nucleotide differences between clades and sequence types. ITS1 sequences from 3 *Marteilia* species were included as the most closely related available sequences as the outgroup

An 18S rRNA gene Bayesian phylogeny of the currently known extent of paramyxid diversity, based on that of Ward et al. (2016), is shown in Fig. 7. An identical topology was retrieved from RAxML analysis. Representative sequence types of *P. canceri* and *P. orchestiae* generated in this study are shown in bold, and formed a maximally supported clade with a *Paramarteilia*-like sequence from filtered water from a *Mytilus edulis* incubation (Ward et al. 2016). The *P. canceri* and *P. orchestiae* sequences differed consistently from each other (as determined from 10 crab-derived sequences: 9 *N. puber* and 1 *C. pagurus*, and 14 amphipod-derived sequences from English samples) at 2 positions across a 683 bp alignment region. With reference to JQ673484 (= *P. orchestiae*) these are: position 722: *P. orchestiae* T, *P. canceri* C; and position 733: *P. orchestiae* G, *P. canceri* C. A possible third difference is at position 961 where the 9 *Necora*-derived sequences have a T and *P. orchestiae* has a C; however, this region is not covered by the *Cancer*-derived sequence.

The 18S sequence of the microsporidian detected in this study differed from the sequence of *Ameson pulvis* (KC456966) at only 2 positions across an 860 bp aligned region. These differences were apparent in sequences from *N. puber* that were generated independently from 3 different infected individuals. Based on this analysis, we conclude that *N. puber* is a host of *A. pulvis* (or a very close relative) previously described infecting the European shore crab (Stentiford et al. 2013). Fig. 8 shows an 18S rRNA gene phylogeny of the *Ameson*/*Nadelspora* clade (Microsporidia), showing all currently available sequences in NCBI GenBank plus the *N. puber*-derived sequence generated in this study.

4. DISCUSSION

We report the findings of a preliminary investigation into the health status of *Necora puber* at 3 fishing sites in Ireland (Howth, Galway Bay and Castletownbere), which was prompted by anecdotal industry reports of an on-going decline in the Galway Bay *N. puber* fishery since ca. 2010. There are no official figures to support the reported declines because the majority of *N. puber* landed in Ireland are caught by

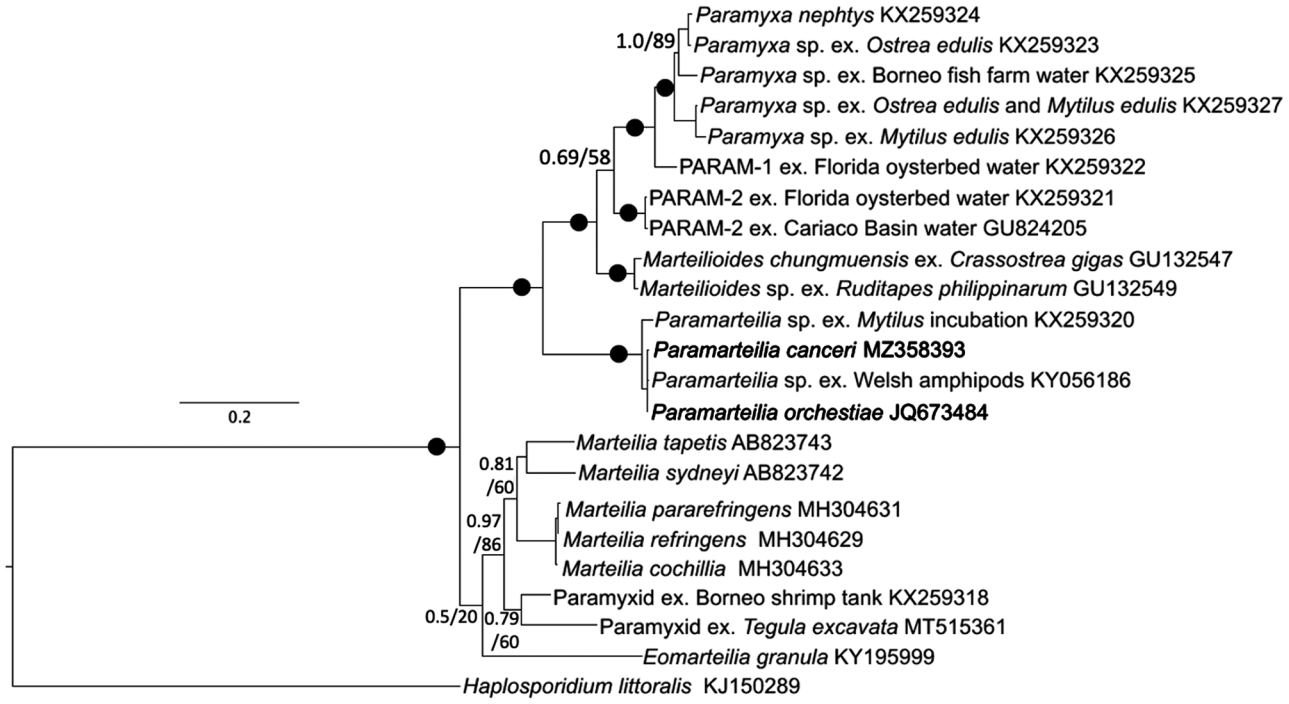

Fig. 7. 18S rRNA gene Bayesian phylogeny of all known paramyxid lineages, including *Paramarteilia orchestiae* and *P. canceri* sequences generated in this study (2M generations) Maximum likelihood analysis (1000 bootstrap replicates) produced an identical topology. Bayesian posterior probability values and maximum likelihood bootstrap values are indicated at each node. Filled black circles represent combined support values of >0.95/95%

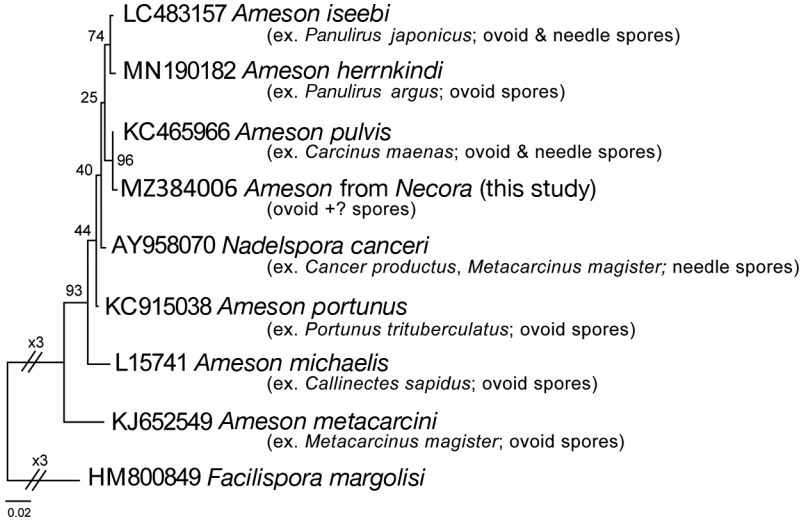

Fig. 8. 18S rRNA gene maximum parsimony phylogeny (1000 bootstrap replicates; bootstrap percentages given at nodes) of all *Ameson*- and *Nadelspora*-annotated sequences in GenBank, plus the *Necora*-infecting *Ameson* sp. from this study. The analysis used all 38 available informative sites. The host decapod species infected by the microsporidia are indicated, as are the microsporidian spore morphologies observed

fishermen in small inshore vessels and they are not obliged to record landings. Additionally, variable catches have always been a feature of this fishery, and the initial decline was thought to be part of this natural variation. However, despite reduced fishing effort, the fishery in Galway Bay has failed to recover, suggesting that other factors may be responsible. Fishermen commented in 2016 that they were catching mostly juvenile crabs and few adults. In response to the reports from fishermen, this investigation initially commenced with a histopathological survey of crabs sampled from inner and outer Galway Bay, and based on those findings, a follow-up survey of 2 of the other 3 main fishing grounds was carried out the following year. The crabs were collected by fishermen from baited pots and transported to the Marine Institute.

By far the most prevalent parasite detected by histology in all 3 bays surveyed was a *Paramarteilia* sp., with the highest prevalence recorded in crabs from Galway Bay. Histopathology, TEM and molecular taxonomic and phylogenetic analyses confirmed it to be *P. canceri*, originally described infect-

ing *Cancer pagurus* in the English Channel (Feist et al. 2009). *P. canceri* was observed systemically invading various host tissues and organs of all infected crabs, and parasites at all developmental stages were seen. However, crabs appeared externally healthy and did not display obvious lethargy. Granulomas were frequently associated with the presence of *Paramarteilia* cells, suggesting a host response to the parasite. In the lumen of the antennal gland, unidentified concretions intermixed with masses of parasite life stages could often be seen, suggesting a possible mode of transmission of the parasite, if the parasite is excreted in the urine. The general nature of the infection observed in *N. puber* is similar to that observed previously for *P. canceri* in *C. pagurus* (Feist et al. 2009). In this study, we provide the first 18S sequences of crab-infecting *Paramarteilia*, from the *C. pagurus*-infecting type material and from *N. puber* collected in Galway Bay.

Very high 18S rRNA gene sequence similarity was observed between *Paramarteilia* lineages from crabs and amphipods; therefore, this gene cannot reliably be used to discriminate between species. The faster-evolving ITS regions of the rRNA gene array provide greater phylogenetic and taxonomic resolution for determining species and evolutionary relationships than the 18S, and are frequently used as species-level markers for both microbial and multicellular eukaryotes (Boenigk et al. 2012), including other paramyxid species, particularly *Marteilia* spp. (Kerr et al. 2018). We generated ITS1 sequences from as many *Paramarteilia*-infected host samples as were available, and demonstrated that crab- and amphipod-associated sequences differ consistently at 13 sites across the ITS1 region (2.9% of sites analysed, compared to 0.3% of 18S sites analysed). Although there are no standardised percentage sequence identity thresholds for delineating species, this level of sequence difference, consistently observed between multiple independent samples of parasites showing different infection characteristics (in this case host species) is consistent with their designation as separate species. As the *Paramarteilia* lineages infecting *C. pagurus* and *N. puber* were morphologically indistinguishable by histopathology, with variation in the number of tertiary cells being the only difference noted by TEM (but based on insufficient sample numbers to distinguish them), and had identical ITS1 sequences, we confidently assign the parasite of *N. puber* as *P. canceri*. Similarly, we assign the amphipod parasites from Ireland, UK and the type location and host in France as *P. orchestiae.* We make no assumption that these crab and amphipod species are the only hosts of *P. canceri* and *P. orchestiae*, respectively. However, our results suggest that the frequently found and widespread *Paramarteilia* infecting amphipods, i.e. *P. orchestiae*, is not the same species of parasite that we associated in this study with disease in velvet crabs, i.e. *P. canceri*, which was originally described by Feist et al. (2009) in *C. pagurus*. Therefore, we do not consider amphipods as a potential reservoir of parasites causing disease in velvet crabs.

Molecular phylogenetics identified the microsporidian co-infecting some *N. puber* individuals as *Ameson pulvis*, or a very close relative (as our 3 independently generated 18S sequences differed at 1 position from the existing *A. pulvis* sequence, itself generated from multiple infections). *A. pulvis* was originally described from the shore crab *Carcinus maenas* (Vivarès & Sprague 1979), and sequenced from that host by Stentiford et al. (2013). The genera *Ameson* and *Nadelspora*, originally distinguished by having ovoid and needle-shaped spores, respectively, are very closely related, and based on available sequence data (18S only) are not phylogenetically distinct. Further confusing the relationship, *A. pulvis* and *A. iseebi* from the Japanese spiny lobster *Panulirus japonicus* produce both ovoid and needle-shaped spores. After inspecting all available histological samples from this study, we observed pathological changes within the heart muscle which are suggestive of the presence of needle-like spores, but this could not be confirmed via TEM. TEM of skeletal muscle identified oval spores, but needle-like spores were not observed within this tissue. However, the production of both spore types may occur under particular conditions, but as they are unknown they cannot be experimentally selected or induced to more rigorously test the phylogenetic distribution of the polymorphic spore character.

The development of the *N. puber* fishery in both Ireland and the UK was driven by sudden declines in fisheries in France and Southern Europe attributed to a combination of over-exploitation and disease. A *Hematodinium* species, the causative agent of 'Pink Crab Disease' (Stentiford et al. 2002), was identified in a survey of French fishing grounds in the 1980s and believed to have been a significant factor in observed declines there (Wilhelm & Mialhe 1996). *Hematodinium* sp. has previously been reported as being prevalent in the 3 main Irish brown crab fisheries in NW, SE and SW Ireland (Robinson et al. 2005, Tully et al. 2006), although previous reports of *Hematodinium* sp. in *N. puber* from the Donegal fishery observed the parasite in only 2 haemolymph smears from 2201 individuals sampled in June 2006 (Ní Chualáin 2010).

The preliminary histological investigation in the present study was carried out to assess the health status of *N. puber* sampled from 3 of the 4 main fisheries, and to establish a baseline of parasites present. *Hematodinium* sp. was detected by histology in *N. puber* collected from all 3 bays sampled, representing the first histological record of *Hematodinium* sp. in *N. puber* from Ireland. Although *Hematodinium* was mostly detected at low frequency in this study, its prevalence was higher than that previously recorded in *N. puber* in Ireland. It is worth noting that Robinson et al. (2005) strongly recommended that a monitoring programme for the *N. puber* and *C. pagurus* fisheries, particularly in relation to *Hematodinium* sp., should be established to protect and conserve both fisheries. It is clear now from this study that *Hematodinium* sp. is present in the western, eastern and southern and probably also in northern velvet crab fisheries.

The intensity and prevalence of *P. canceri* in *N. puber* sampled from Galway Bay was an unexpected finding and prompted the further sampling of the other velvet crab fisheries. Further investigations are required to ascertain whether prevalences of *P. canceri* are generally lower in Castletownbere and Howth than in Galway Bay; whether infection prevalence and intensity are related to host size, sex or injury; and to what extent *P. canceri* causes mortality in *N. puber*. The intensity and prevalence of infection of *N. puber* by *P. canceri* in Galway Bay suggest that its presence may play a role in the reported declines in catches of velvet crabs in that area (potentially compounded by other co-infecting parasites). The potential significance of the pathogens identified in this study strongly suggests that a surveillance programme should be established encompassing all potential pathogens of *N. puber*. The possibility of a complex aetiology of disease in *N. puber* involving *P. canceri*, *Hematodinium* and possibly other microbes and environmental factors, is also worthy of further investigation.

Acknowledgements. G.M.W. was supported by a Natural Environment Research Council GW4+ Doctoral Training Programme PhD studentship held at The University of Exeter, UK, The Natural History Museum (NHM), UK, and Centre for Environment, Fisheries and Aquaculture Science (Cefas), UK; the work was also supported by funding from the UK Department of Environment, Food and Rural Affairs (Defra) under contract FC1214 and FC1215 (to D.B., K.S.B. and A.U.), FX001 (to G.D.S.) and FB002A (to S.W.F.). We thank the members of the Marine Institute – Fish Health Unit for their contribution to this project and Sinead O'Brien for assistance in the collection of crabs.

LITERATURE CITED

Bakir WMA, Healy B (1995) Reproductive cycle of the velvet swimming crab *Necora puber* (L.) (Decapoda, Brachyura, Portunidae) on the east coast of Ireland. Irish Fisheries Investigations Services B, Department of the Marine, Dublin

Boenigk J, Ereshefsky M, Hoef-Emden K, Mallet J, Bass D (2012) Concepts in protistology: species definitions and boundaries. Eur J Protistol 48:96–102

Christiansen ME (1969) Decapoda Brachyura. Marine invertebrates of Scandinavia 2. Universitetsforlaget, Oslo

Davies CE, Bass D, Ward GM, Batista FM and others (2020) Diagnosis and prevalence of two new species of haplosporidians infecting shore crabs *Carcinus maenas: Haplosporidium carcini* n. sp., and *H. cranc* n. sp. Parasitology 147:1229–1237

Feist SW, Bateman KS, Longshaw M, Stentiford GD, Hine M (2009) *Paramarteilia canceri* n. sp. (Paramyxea: Marteiliidea) in the European edible crab (*Cancer pagurus*). Folia Parasitol 56:73–85

Ginsburger-Vogel T (1991) Intersexuality in *Orchestia mediterranea* Costa, 1853, and *Orchestia aestuarensis* Wildish, 1987 (Amphipoda): a consequence of hybridization or parasitic infestation? J Crustac Biol 11:530–539

Ginsburger-Vogel T, Desportes I (1979) Étude ultrastructurale de la sporulation de *Paramarteilia orchestiae* gen. n., sp. n., parasite de l'amphipode *Orchestia gammarellus* (Pallas). J Protozool 26:390–403

Ginsburger-Vogel T, Desportes I, Zerbib C (1976) Présence chez l'amphipode *Orchestia gammarellus* (Pallas) d'un protiste parasite, ses affinités avec *Marteilia refringens* agent de l'épizootie de l'huître plate. C R Acad Sci Paris 293:939–942

Gouy M, Guindon S, Gascuel O (2010) SeaView version 4: a multiplatform graphical user interface for sequence alignment and phylogenetic tree building. Mol Biol Evol 27:221–224

Katoh K, Standley DM (2013) MAFFT multiple sequence alignment software version 7: improvements in performance and usability. Mol Biol Evol 30:772–780

Kerr R, Ward GM, Stentiford GD, Alfjorden A and others (2018) *Marteilia refringens* and *Marteilia pararefringens* sp. nov. are distinct parasites of bivalves and have different European distributions. Parasitology 145:1483–1492

Marine Institute, Bord Iascaigh Mhara (2019) Shellfish stocks and fisheries review 2019: an assessment of selected stocks. Marine Institute, Galway

Miller MA, Pfeiffer W, Schwartz T (2010) Creating the CIPRES science gateway for inference of large phylogenetic trees. In: 2010 Gateway Computing Environments Workshop, New Orleans, LA, p 1–8. doi:10.1109/GCE.2010.5676129

Ní Chualáin C (2010) Impacts of the parasitic dinoflagellate *Hematodinium* sp. on Irish crustacean fisheries. PhD thesis, Galway-Mayo Institute of Technology, Galway

Parker JD, Warner MC (1970) Effects of fixation, dehydration and staining on dimensions of myxosporidan and microsporidan spores. J Wildl Dis 6:448–456

Pickup J, Ironside JE (2018) Multiple origins of parasitic feminization: thelygeny and intersexuality in beachhoppers are caused by paramyxid parasites, not microsporidia. Parasitology 145:408–415

Reynolds ES (1963) The use of lead citrate at high pH as an

electron-opaque stain in electron microscopy. J Cell Biol 17:208–212

Robinson M, Hayes M, Allen B, Thorne K, Jenkins E, Stafford P (2005) Monitoring the prevalence of the parasitic dinoflagellate *Hematodinium* in Irish brown crab fisheries. Report of Project No. 04.SM.T1.04. National Development Plan: Supporting Measures for Sea Fisheries Development. https://www.vims.edu/research/departments/eaah/programs/crustacean/research/hematodinium/literature/pdf%20files%202/Robinson%20et%20al.%202005%20REPORT.pdf

Ronquist F, Teslenko M, van der Mark P, Ayres DL and others (2012) MrBayes 3.2: efficient Bayesian phylogenetic inference and model choice across a large model space. Syst Biol 61:539–542

Short S, Guler Y, Yang G, Kille P, Ford AT (2012) Paramyxean–microsporidian co-infection in amphipods: Is the consensus that microsporidia can feminise their hosts presumptive? Int J Parasitol 42:683–691

Stamatakis A (2014) RAxML version 8: a tool for phylogenetic analysis and post-analysis of large phylogenies. Bioinformatics 30:1312–1313

Stentiford GD, Green M, Bateman KS, Small HJ, Neil DM, Feist SW (2002) Infection by a *Hematodinium*-like parasitic dinoflagellate causes Pink Crab Disease (PCD) in the edible crab *Cancer pagurus.* J Invertebr Pathol 79: 179–191

Stentiford GD, Bateman KS, Feist SW, Chambers E, Stone DM (2013) Plastic parasites: Extreme dimorphism creates a taxonomic conundrum in the Phylum Microsporidia. Int J Parasitol 43:339–352

Stentiford GD, Ross S, Minardi D, Feist SW and others (2018) Evidence for trophic transfer of *Indosporus octospora* and *Ovipleistophora arlo* n. sp. (Microsporidia) between crustacean and fish hosts. Parasitology 145:1105–1117

Tully O, Robinson M, O'Keeffe E, Cosgrove R, Doyle O, Lehane B (2006) The brown crab (*Cancer pagurus* L.) fishery: analysis of the resource in 2004–2005. Fish Res Ser No. 4. Bord Iascaigh Mhara, Dublin

Urrutia A, Bass D, Ward G, Ross S, Bojko J, Marigomez I, Feist SW (2019) Ultrastructure, phylogeny and histopathology of two novel haplosporidians parasitising amphipods, and importance of crustaceans as hosts. Dis Aquat Org 136:87–103

Vivarès CP, Sprague V (1979) The fine structure of *Ameson pulbis* (Microspora, Microsporidia) and its implications regarding classification and chromosome cycle. J Invertebr Pathol 33:40–52

Ward GM, Bennett M, Bateman K, Stentiford GD and others (2016) A new phylogeny and environmental DNA insight into paramyxids: an increasingly important but enigmatic clade of protistan parasites of marine invertebrates. Int J Parasitol 46:605–619

Wilhelm G, Mialhe E (1996) Dinoflagellate infection associated with the decline of *Necora puber* crab populations in France. Dis Aquat Org 26:213–219

Editorial responsibility: Jeffrey Shields, Gloucester Point, Virginia, USA
Reviewed by: 3 anonymous referees

Submitted: July 2, 2021
Accepted: January 14, 2022
Proofs received from author(s): April 8, 2022